

Chapter 4

Electromechanical Impedance Based Crack Detection for a Rotating Machine

Aldemir Ap Cavalini Jr, Roberto Mendes Finzi Neto, and Valder Steffen Jr

Abstract Visual examination, ultrasonic tests, and dye penetrant inspection, are some examples of nondestructive techniques widely used for crack detection in rotors. These methods have proved to be costly, since satisfactory results rely on detailed and periodic inspections. Significant research effort has been directed in recent years to online monitoring techniques, i.e., based on vibration signals measured during rotor operation. However, most of them are able to only detect deep cracks. The uniqueness of this paper relies on the detection of incipient transverse cracks in rotating shafts by using the so-called, electromechanical impedance method. This method has become a promising tool for structural health monitoring of machines due to its sensitivity to small local damage. Basically, the method monitors changes in the electric impedance of piezoelectric transducers, bonded to (or embedded into) the host structure, through specific mathematic functions, the so-called damage metrics, to detect damage. This is possible because the transducer's impedance is directly related to the mechanical impedance of the structure. In this context, successful experimental tests were performed in a horizontal rotor supported by roller bearings. PZT patches were bonded along the rotor's shaft, in which transverse cracks were introduced. The technique was validated under different unbalance conditions.

Keywords SHM technique • Rotating machine • Crack detection • Electromechanical impedance method • Catastrophic failures

4.1 Introduction

According to [1], shaft crack detection is a very serious matter, and machines that are suspected of having a crack must be treated with the upmost respect. The importance attributed to this problem is addressed to the serious consequences when cracks are not early identified in rotating systems. In 1987 [2], Allianz, a consolidated insurance company, organized a conference about the prevention of catastrophic failures in rotating machinery. During this event, 37 cases of crack detection were reported to have occurred only in Europe after 1967. Additionally, 16 cases of catastrophic failure were presented, being some of them credited to the presence and propagation of transverse cracks. Accidents of this magnitude are usually kept in secret by the manufacturers. However, documented information shows that cracks have been detected continuously in steam turbines, generators, and pumps of industrial plants in Europe, North America, etc.

Although there are no statistical studies that account for the exact dimension of the damage caused by cracks in rotating shafts, the Electric Power Research Institute estimates that approximately \$1 billion were expended in repairs, exchanges, loss of production, etc., in electrical industries, nuclear, and conventional, since the 1970s [3]. Thus, manufacturers have adopted design concepts (shafts manufactured with materials that have high values of fracture toughness on the operation temperature), as well as, special procedures for startup, operation, monitoring, and maintenance, in order to minimize the appearance and grown of cracks in different rotors, such as, steam turbines, centrifugal compressors, and generator units found in hydroelectric plants.

A.A. Cavalini Jr (✉) • R.M. Finzi Neto • V. Steffen Jr
LMEst - Structural Mechanics Laboratory, INCT (EIE) - National Institute of Science and Technology, Federal University of Uberlândia, School of Mechanical Engineering, Av. João Naves de Ávila 2121, Uberlândia, MG 38408-196, Brazil
e-mail: aacjunior@mecanica.ufu.br

There are several structural monitoring techniques, the so-called SHM techniques, proposed in the literature for crack detection in rotating machines. Among them, the ones based on vibration measurements are recognized as useful tools because they lead to satisfactory results even when the damage location is not accessible or even unknown [4]. About these kind of techniques, two accepted rules are employed for detecting a crack. The first one is based on the monitoring of the synchronous vibration amplitude and phase. According to [1], changes in $1\times$ amplitude and phase are the primary indicators of crack presence. The second rule relies on $2\times$ vibrations, where [1] states that if a cracked rotor has a steady unidirectional radial load, then a strong $2\times$ response may appear when the rotor is turning at half of any balance resonance speed. However, although widely used in industry, when applied in non-ideal conditions such techniques can detect cracks that eventually have already spread significantly by the cross section of the shaft, usually above 40 % of its diameter. Therefore, currently, the researchers' attention is turning to more sophisticated methods capable of identifying incipient cracks (cracks that spread up to 25 % of shaft diameter), which represent a type of damage that are hardly observable in vibration analysis.

In this context, the aim of this paper relies on the detection of incipient transverse cracks in rotating shafts by using the so-called electromechanical impedance method. This technique measures the electromechanical impedance of the structure by using patches of piezoelectric material (PZT patches) bonded on the surface of the structure (or embedded into it). Through the PZT sensor-actuators, the electromechanical impedance, which is directly related to the mechanical impedance of the structure, is obtained. Based on changes of the impedance signals (e.g., due to the growing crack), the damage can be detected. Damage metrics are normally used to quantify the severity of the failure [5]. The electromechanical impedance method has advantages over other SHM techniques [6]. The mathematical model of the structure is not required, which allows the application of the proposed technique in complex systems. Additionally, the results generated by the technique are easily to interpret and they are prone to be adapted to continuous monitoring. This SHM technique operates at high frequencies as compared to the range of frequencies that are normally used in modal analysis (sensitive to incipient damage). The PZT patches have a wide linearity range, being lightweight and durable. Consequently, this method is extensively applied to damage detection, particularly in aircraft structures. In [7], an extensive literature review is available regarding various applications of this technique.

It is important to point out that no reports were found in the available databases on the application of the electromechanical impedance method in rotating systems, which makes this proposal quite unique in the area of rotor dynamics. There are particularities specific to the application of the method in rotor systems. For example, the rotor is dynamically excited. In most studies about crack detection by using the electromechanical impedance method, the impedance signatures are measured with the structure at rest. Another particularity is related to the device that enables the acquisition of the impedance signal when the rotor is in operation. Clearly, in this type of application electrical signals have to be transmitted by electric cables from the rotating shaft to a fixed measurement system (and vice versa) with little interference of noise even when the rotor is operating at high speeds. These special features will be discussed along this work.

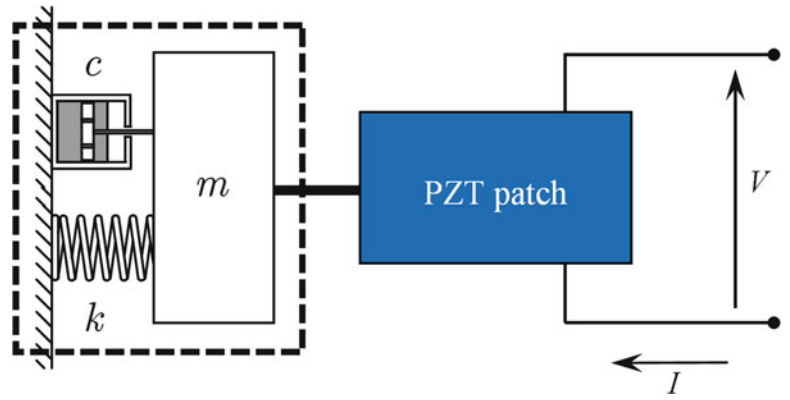
4.2 Impedance Based Structural Health Monitoring

The impedance based SHM technique was first proposed by [8], and subsequently the method was extended by many other researches [9–15]. As mentioned, this technique uses small PZT patches (impedance sensors) to monitor changes in the structure that may occur due to the appearing of damage (changes in stiffness, damping, and mass). When the PZT is bonded to the structure and a low electric voltage is applied, generally 1V [16], a strain is produced. Using a high excitation frequency (in terms of typical modal analysis testing), the dynamic response of the structure will represent only the local area around the sensor. The dynamic response of the induced mechanical vibrations is transmitted by the same PZT patch as an electrical signal. Thus, if an incipient damage was grown in the system, changes can be observed in the electric response measured by the PZT (dynamic response that leads to an impedance signature). The electromechanical model that quantifies and describes the measurement process is illustrated in Fig. 4.1 for a single degree of freedom system (mass m , stiffness k , and damping c ; V and I are the voltage and current, respectively).

For this system, [8] demonstrated that the admittance $Y_a(\omega)$ (inverse of the impedance) of the PZT patch can be written as a function of the combined PZT actuator and structure mechanical impedances, $Z_{ma}(\omega)$ and $Z_{me}(\omega)$, respectively, as given by Eq. (4.1):

$$Y_a(\omega) = I(\omega) \omega a \left\{ \varepsilon_{33}^T [1 - I(\omega) \delta] - \frac{Z_{ma}(\omega)}{Z_{ma}(\omega) - Z_{me}(\omega)} d_{3x}^2 \widehat{Y}_{xx}^E \right\} \quad (4.1)$$

Fig. 4.1 Electromechanical model that describes the process of measuring the impedance signature



where \hat{Y}_{xx}^E is the complex Young's modulus of the PZT with zero electric field, d_{3x} is the piezoelectric coupling constant in the arbitrary x direction at zero electric field, ε_{33}^T is the dielectric constant at zero stress, δ is the dielectric loss tangent to the PZT, a is a geometric constant of the PZT, and is ω the frequency. Assuming that the mechanical properties of PZT do not vary over time used for monitoring, Eq. (4.1) shows that the electrical impedance of the PZT patch is directly related to the structure's impedance (damages cause changes in the structure's mechanical impedance). As shown in Eq. (4.1), the impedance is a complex function of the frequency having real and imaginary parts. The real part is more sensitive to structural changes, i.e., it is the most suitable for the detection of damage [17].

Extensively applied in different structures, particularly in aircrafts, the electromechanical impedance method operates at high frequencies (typically ranging from 30 to 250 kHz, determined by a trial and error method) and has an accurate sensitivity to incipient damage [18]. According to [7], for a simple PZT patch, a damage located at a distance up to 0.4 m can be identified in composite materials and up to 2 m in bars consisting of a single metal. The impedance signature is determined by means an impedance analyzer. The structural integrity assessment is made based on the comparison of impedance signatures measured before and after the occurrence of a possible damage. A visual comparison is not enough, being necessary to use quantitative criteria. In this sense, the so-called damage metrics is defined, which is represented by scalar parameters that are able to represent numerically the difference between two measurements. Among the various damage metrics proposed, the root mean square (RMS), the deviation of the root mean square (RMSD), and the deviation of the correlation coefficient (CCD), are the mostly used.

As the first damage metric, Eq. (4.2) defines the root mean square (RMS).

$$RMS = \left\{ \sum_{i=1}^n \frac{[\text{Re}(Z_{1i}) - \text{Re}(Z_{2i})]^2}{n} \right\}^{1/2} \quad (4.2)$$

where $\text{Re}(Z_{1i})$ is the real part of the impedance signature of the system without damage (reference value: *Baseline*) and $\text{Re}(Z_{2i})$ is the real part of the impedance signature of the system for an unknown structural condition, n is the number of points (frequency vector) of the impedance signal ($i = 1, 2, \dots, n$).

The deviation of the root mean square (RMSD) is given by Eq. (4.3). This metric is not qualitatively affected when applied in impedance signatures obtained from different PZT patches (different amplitude levels).

$$RMSD = \left\{ \sum_{i=1}^n \frac{[\text{Re}(Z_{1i}) - \text{Re}(Z_{2i})]^2}{\text{Re}(Z_{1i})^2} \right\}^{1/2} \quad (4.3)$$

The deviation of the correlation coefficient, CCD, is used to measure and interpret the information found in both data sets considered. The mathematical formulation of this metric is given by the difference between the first scale and the correlation coefficient CC of the signatures obtained from any measurement and its reference [19]. The greater the correlation coefficient, CC , the smaller will be the deviation CCD and smaller are the changes caused by the damage in the system.

$$CCD = 1 - CC = 1 - \frac{1}{n} \sum_{i=1}^n \frac{[\text{Re}(Z_{1i}) - \text{Re}(\bar{Z}_{1i})] - [\text{Re}(Z_{2i}) - \text{Re}(\bar{Z}_{2i})]}{S_{Z1} S_{Z2}} \quad (4.4)$$

where $Z_{1,i}$ is the impedance of the PZT patch measured at healthy conditions, $Z_{2,i}$ is the impedance for the comparison with the *baseline* measurement at frequency interval i . The symbols \bar{Z}_{1i} and \bar{Z}_{2i} represent mean values, while S_{Z1} and S_{Z2} represent standard deviations.

4.3 Experimental Results

Figure 4.2 shows the test rig used in the application of the SHM technique proposed by this work, i.e., the detection of incipient transverse cracks in rotating shafts by using the electromechanical impedance method. This machine is composed by a flexible steel shaft with 860 mm length and 17 mm diameter, and two rigid discs, both of steel with 150 mm diameter and 20 mm thickness (approximately 2.65 kg each). The shaft is supported by two roller bearings, one of them is a hybrid bearing with electromagnetic actuators (not used in the present contribution). The system is driven by a DC electric motor of 0.5 CV (*Varimot*[®] model BN90M). Its angular position is monitored by means of an encoder (coupled to the free end of the DC electric motor), which is able to produce 1 or 720 pulses per revolution of the shaft (*Suprasonic*[®] model CSS58C-6). The interaction between the electric motor and the shaft is minimized by means of a special coupling named *Lami-Torq* (*Acoplast*[®] model GTG 402 100). From a representative mathematical model of the rotor (finite element model), the first two critical speeds were determined, being approximately: 1,685 rev/min (28.1 Hz) and 5,430 rev/min (90.5 Hz).

As mentioned, the electromechanical impedance method is able to detecting the presence of structural defects at a distance up to 2 m from the PZT patch (simple beam metal without barriers). Clearly, this is not the case of the rotor shown in Fig. 4.2 (three sections limited by the discs). Thus, four PZT patches (12×6 mm) were distributed along the shaft placed at 90° from each other to cover the largest possible surface for detection. For this aim, four machining processes as show in Fig. 4.3 were performed.

An extra PZT (15×15 mm) was coupled to the side of one disc to investigate if sensors orthogonal to the damage are able to detect the failures. This becomes interesting because, if successful, it would not be necessary to perform the machining on the shaft surface. Of course, the above machining process is a drawback of the method (e.g. in industrial machines the PZT patch may be coupled to pulleys). The PZT coupling was performed by using the glue *REPSOL*[®], selected for its good adhesion (piezoelectric patches to steel structures). Figure 4.4 shows a schematic arrangement with each of the five patches bonded to the system, namely PZT-1, PZT-2, PZT-3, PZT-4, and PZT-D (numbered starting from the hybrid bearing; B_1 in Fig. 4.3).

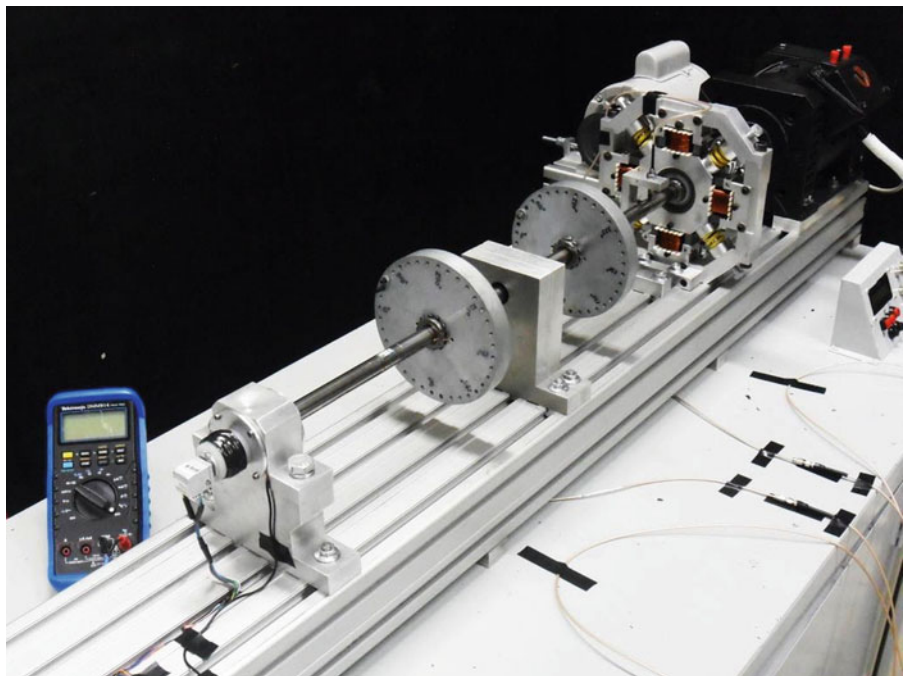


Fig. 4.2 Test rig used in the application of the electromechanical impedance method

Fig. 4.3 Machining process performed on the shaft surface to allow the coupling of the PZT patches



Fig. 4.4 Distribution of the PZT patches along the shaft and on the face of the disc (dimension in mm; note that this scheme is reversed from the picture of Fig. 4.2)

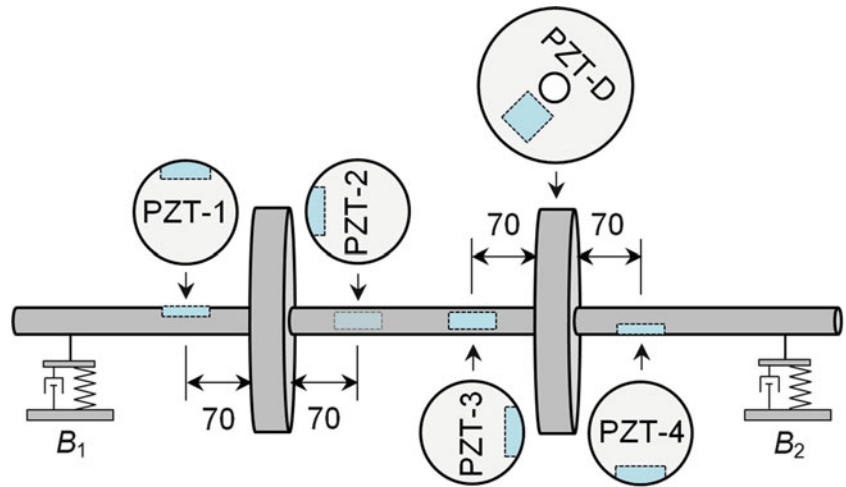
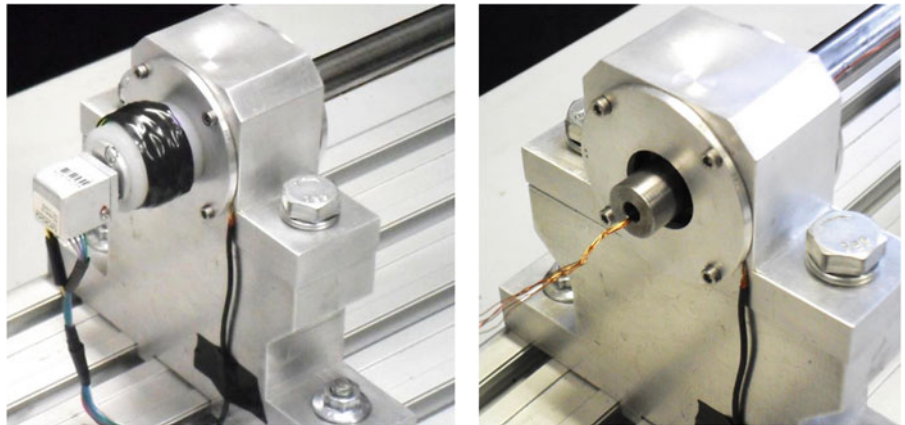


Fig. 4.5 Slip ring connected to the shaft end through the nylon device



For the measurement of the impedance signatures of the PZT patches with the test rig under operation condition (sending excitation signals to the PZT patches and acquiring the responses), a slip ring was used (*MOOG*[®] model EC3848-10). This device is able to transfer electrical signals from fixed to rotating parts (and vice-versa) with low noise interference, even with the rotor operating at high speeds (according to the manufactures, the device is able to transfer electrical signals from accelerometers with the rotor operating in a range of 0–10,000 rev/min). Figure 4.5 shows the slip ring connected to one of the shaft ends. Note that a nylon device was used for coupling the parts. Also, for the sake of clarity, a figure showing the slip ring before assemblage to the shaft can be seen.

Using a low-cost impedance measurement system [20], with the rotor at rest, a frequency sweep was applied to each PZT patch in the range between 0 and 200 kHz for determining the regions with the greatest number of peaks in the impedance signature. Only two evident peaks were found in the impedance signature of the sensors coupled to the shaft (signatures

Table 4.1 Frequency bandwidths used for each one of the five PZT patches

PZT	Frequency bandwidth (kHz)	
	From	To
1	169.1	170.2
2	168.6	169.8
3	168.6	169.8
4	168.7	170.2
D	170	180

Fig. 4.6 Details about the position of DAMAGE-1 in the shaft

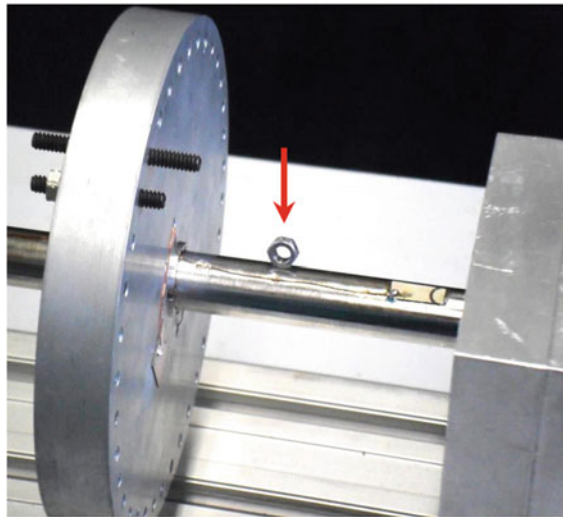
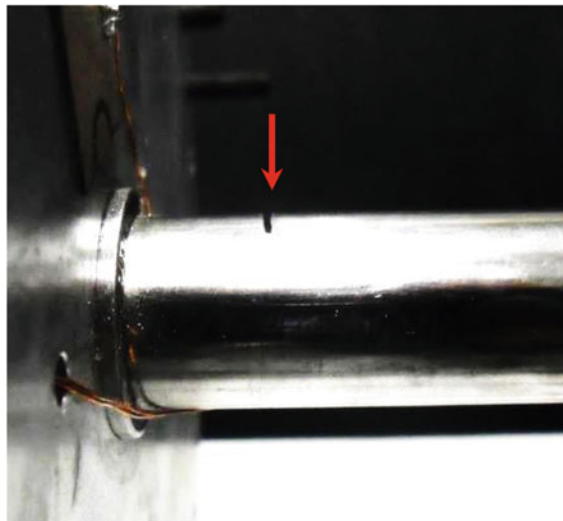


Fig. 4.7 Details of the saw cut performed on the shaft to simulate the crack (DAMAGE-2)

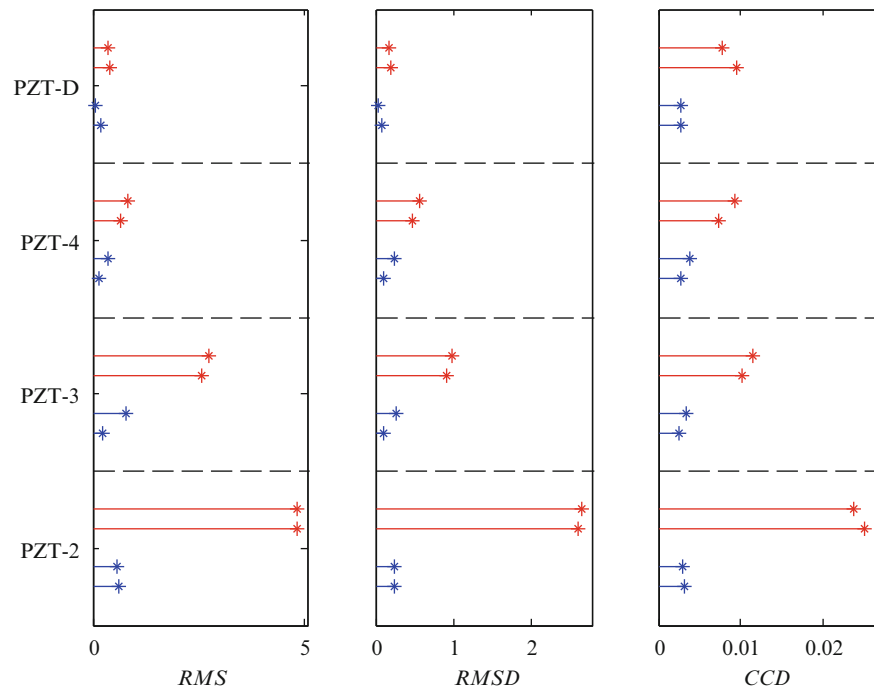


with 401 frequency points). Only the PZT attached to the disc showed more peaks, a result that is typically found in thick plates. Table 4.1 shows the frequency bandwidths determined. Note that the bands are delimited at high frequencies, which, as previously mentioned, allows for detecting incipient damage.

The tests with the proposed methodology included the analysis of two incipient structural damages. In the first one (DAMAGE-1), a steel nut was bonded on the shaft surface (mass of 1.06 g) at approximately 30 mm from one of the discs (40 mm from PZT-3; region delimited by the discs). This nondestructive damage (structural modification) was inserted to perform a preliminary evaluation of the proposed technique. Figure 4.6 shows the positions of PZT-3 and PZT-D, concerning the damage DAMAGE-1.

The second analysis, DAMAGE-2, is a destructive damage. In this case, a saw cut was performed along the shaft cross-section by using a thin machining disc to simulate a crack. This was done about 15 mm from one of the discs (55 mm from PZT-3; region delimited by the discs). The machining work led in a “crack” of approximately 0.5 mm thick and 2.5 mm depth (about 15 % over the shaft diameter), as shown in Fig. 4.7.

Fig. 4.8 Damage metric values obtained with the rotor balanced and operating at 1,200 rev/min for two different structural conditions: undamaged (*blue line*) and DAMAGE-1 (*red line*) (Color figure online)



In the analysis of both presented damages, the rotor was kept under 1,200 rev/min. However, two different unbalanced conditions were considered: balanced rotor (balancing performed by using the method of influence coefficients) and unbalanced rotor by 306 g mm/ -50° inserted on both discs (identic unbalances in both disks). Different operating speeds were evaluated, leading to similar results (not presented here). The impedance signals were calculated from an average of 10,000 measurements. In addition, a total time of 0.46154 s was used to measure the 10,000 signals related to each one of the 401 frequencies comprising the impedance signatures. This high number of measurements actually reduces the incidence of “noise” that arises from the dynamic behavior of the rotor (together with some electrical effects).

It is known that the variation of temperature may prejudice the results obtained by the electromechanical impedance method. In addition to the environmental temperature effects, specifically for this application, a temperature variation occurs due to the operation of the rotating machine. These effects are more pronounced in the regions close to the bearings (bearings acting as sources of friction). Of course, the temperature varies until stabilization (temperature increases with the rotational speed of the rotor). To minimize this problem, at each round of testing the rotor was kept under the same operation conditions for 60 min before initiating the measurement procedure. In both tests, the room temperature was controlled in the range between 18 and 21 °C.

Figure 4.8 shows the damage metrics obtained for the structural conditions of the rotor without damage and DAMAGE-1, considering the rotor balanced (remember that in all tests the rotor was in operation at 1,200 rev/min). Note that for all the damage metrics analyzed (*RMS*, *RMSD* or *CCD*), the sensors PZT-2 and PZT-3 were the best to detect DAMAGE-1. The PZT-D was not able to detect clearly the imposed damage. It is possible to observe that even PZT-4 was able to detect DAMAGE-1 (PZT apart from the damage by one disc). The results obtained from PZT-1 were discarded because this sensor presented incoherent results during the tests. Figure 4.9 shows the damage metrics determined when the conditions without damage were analyzed (the same results shown in Fig. 4.8) and the damage DAMAGE-2 (saw cut performed on the shaft surface; Fig. 4.7), considering the rotor balanced. Note that in all cases the damages could be detected satisfactorily. Analyzing Fig. 4.9, it can be seen that PZT-3 showed smaller variation from the *baseline* (reference condition; rotor without damage) than PZT-2, which are closer to the DAMAGE-2 (see Fig. 4.7). This leads to the conclusion that there is a difference involving the electromechanical coupling of these PZT patches with the shaft (probably due to the glue adhesion).

Figure 4.10 shows the impedance signatures measured by the PZT-3 determined for the rotor operating under each structural condition (according to the results shown in Figs. 4.8 and 4.9). Note that the largest deviation from the reference curve (*baseline*) occurs for the signature related with DAMAGE-1. The variation caused by the saw cut (DAMAGE-2) is small, an effect confirmed by the damage metrics shown in Fig. 4.9 (compare with Fig. 4.8). The impedance signatures obtained from other PZTs exhibit similar behavior.

Fig. 4.9 Damage metric values obtained with the rotor balanced and operating at 1,200 rev/min for two different structural conditions: undamaged (blue line) and DAMAGE-2 (green line) (Color figure online)

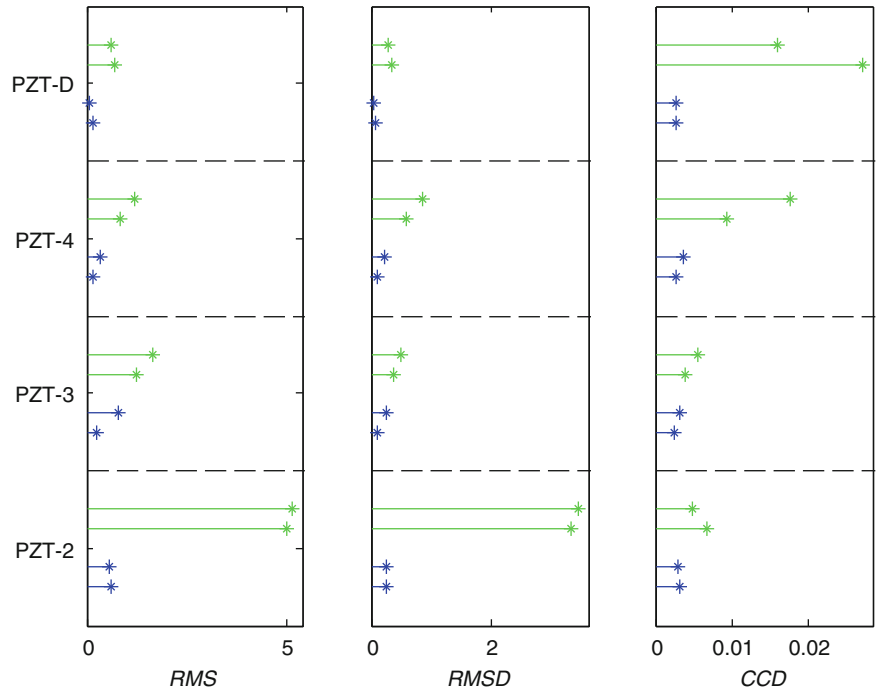
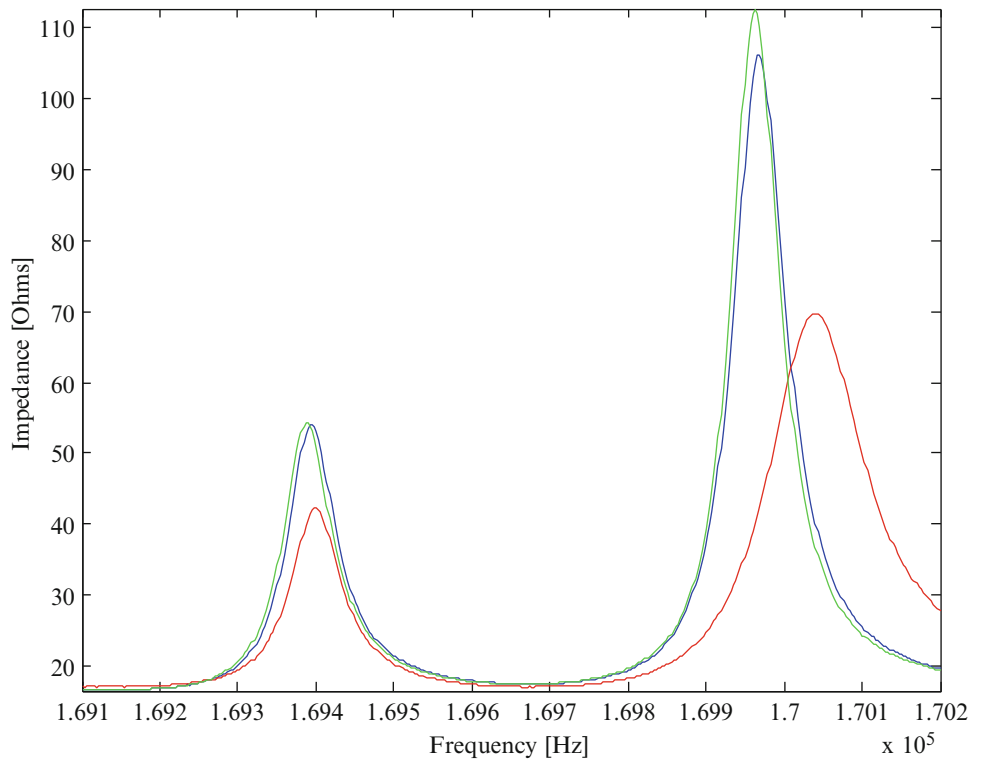


Fig. 4.10 Impedance signatures acquired by the PZT-3 with the rotor balanced and operating at 1,200 rev/min for all structural conditions: undamaged (blue line), DAMAGE-1 (red line), and DAMAGE-2 (green line) (Color figure online)



However, an interesting result was obtained for the rotor under the unbalanced condition (unbalance masses added to the two discs). The PZT-D began to detect more efficiently the saw cut (DAMAGE-2). Figure 4.11 shows the damage metrics found when the structural conditions of the rotor without damage and DAMAGE-2 were evaluated.

Note the difference in the indices obtained from the PZT-D (mainly for the CCD metric) in this operating condition, with respect to the results presented for the rotor under a balanced condition (Fig. 4.9). This result is addressed to the increasing

Fig. 4.11 Damage metric values obtained for the rotor unbalanced and operating at 1,200 rev/min for two different structural conditions: undamaged (*blue line*) and DAMAGE-2 (*green line*) (Color figure online)

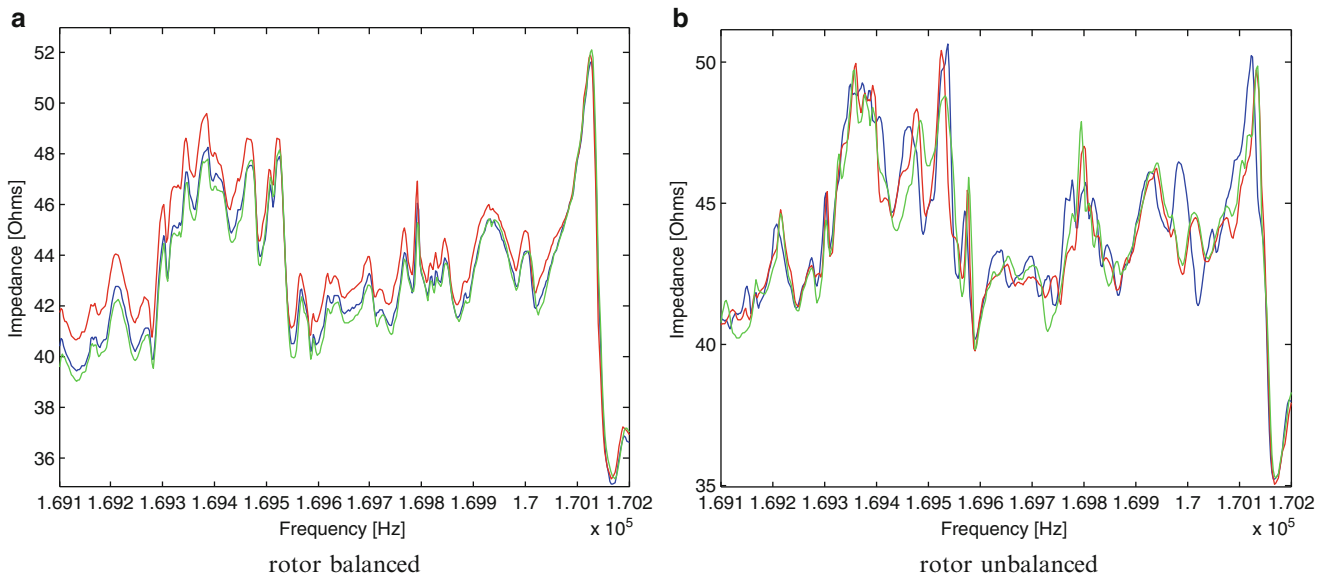
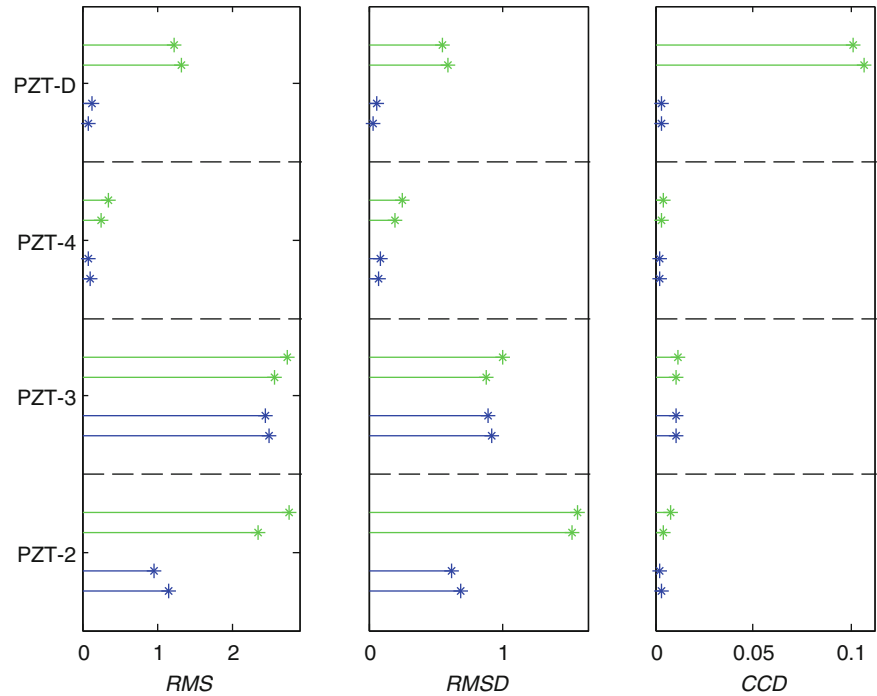


Fig. 4.12 Impedance signatures acquired by the PZT-D for the rotor at 1,200 rev/min for all structural conditions: undamaged (*blue line*), DAMAGE-1 (*red line*), and DAMAGE-2 (*green line*) (Color figure online)

of the vibration of the rotor with the unbalance (the dynamic behavior of the system becomes more significant). Also, note that the results obtained from the other PZT patches are similar to the ones determined for the balanced rotor condition. The DAMAGE-1 was again detected by all the sensors (results not shown here).

Figure 4.12 shows the impedance signatures measured by PZT-D with the rotor balanced (Fig. 4.12a; refers to Figs. 4.8 and 4.9) and unbalanced (Fig. 4.12b; refers to Fig. 4.11) for the three structural conditions. Comparing the curves, one can observe that the changes found in the impedance signatures with damage are more important for the case in which the rotor is unbalanced. This result is also demonstrated by the damage metrics shown in Figs. 4.9 and 4.11.

4.4 Conclusion

The results shown in the present contribution demonstrate the efficiency of the electromechanical impedance method for the detection of incipient cracks in transverse rotating shafts. As seen, the proposed SHM technique was evaluated for the rotor under operation, leading to satisfactory results. The rotordynamic applications were made possible by the use of a special device, the slip ring. In addition, a saw cut was performed on the shaft in order to simulate a crack (procedure adopted by many authors). Attempting to use PZT sensors coupled orthogonally to the shaft (e.g., in pulleys) found limited success. Good results were obtained for the cases in which unbalanced rotors were considered. The effect on the detection capability presented by PZT-D with the increase of the level of unbalance is interesting. Apparently, the variation of local stiffness imposed by the cut is detected more easily when the levels of imbalance are higher, i.e., when the mechanical stresses on the shaft are larger. The high frequency band is an advantage of the method since it permits the detection of incipient damage even in regions of small deflection of the shaft. Most SHM techniques devoted to the detection of cracks in rotors have this limitation. The coupling of the PZT patches to the shaft was made from a machining process, clearly a disadvantage of this application. Thus, in further research work on this topic the use of more flexible piezoelectric sensors is intended (such as Micro Fiber Composites—MFC).

Acknowledgments The authors are thankful to the Brazilian Research Agencies FAPEMIG and CNPq (INCT-EIE) and also to CAPES for the financial support provided for this research effort.

References

1. Bently DE, Hatch CT (2002) Fundamentals of rotating machinery diagnostics. Bently Pressurized Bearing Company, Minden
2. Bachschmid N, Pennacchi P, Tanzi E (2010) Cracked rotors: a survey on static and dynamic behaviour including modelling and diagnosis. Springer, Berlin
3. Sabinavis G, Kirk RG, Kasarda M, Quinn D (2004) Cracked shaft detection and diagnosis. *Shock Vib Dig* 36(4):287–296
4. Carden EP, Fanning P (2004) Vibration based condition monitoring: a review. *Struct Health Monit* 3(5):355–377
5. Palomino LV, Steffen V Jr (2009) Damage metrics associated with electromechanical impedance technique for SHM applied to a riveted structure. In: Proceedings of COBEM2009: 20th international congress of mechanical engineering, Gramado-RS
6. Park G, Inman DJ (2005) Impedance-based structural health monitoring. Damage prognosis for aerospace, civil and mechanical system. Wiley, England, pp 1–12
7. Park G, Sohn H, Farrar CR, Inman DJ (2003) Overview of piezoelectric impedance-based health monitoring and path forward. *Shock Vib Dig* 35(6):451–463
8. Liang C, Sun FP, Rogers CA (1994) Coupled electromechanical analysis of adaptive material systems: determination of the actuator power consumption and system energy transfer. *J Intell Mater Syst Struct* 5:12–20
9. Chaudhry Z, Joseph T, Sun F, Rogers C (1995) Local-area health monitoring of aircraft via piezoelectric actuator-sensor patches. In: Proceedings of the SPIE: SPIE conference, smart structures and integrated systems, vol 2443, San Diego
10. Sun FP, Chaudhry Z, Liang C, Rogers CA (1995) Truss structure integrity identification using PZT sensor-actuator. *J Intell Mater Syst Struct* 6:134–139
11. Park G, Cudney H, Inman DJ (2000) An integrated health monitoring technique using structural impedance sensors. *J Intell Mater Syst Struct* 11(6):448–455
12. Giurgiutiu V, Zagrai A (2000) Characterization of piezoelectric wafer active sensors. *J Intell Mater Syst Struct* 11:959–976
13. Giurgiutiu V, Zagrai AN, Bao J, Redmond J, Roach D, Rackow K (2003) Active sensors for health monitoring of aging aerospace structures. *Int J Cond Monit Diagn Eng Manag* 6(1):3–21
14. Moura JRV Jr, Steffen V Jr (2004) Impedance-based health monitoring: frequency band evaluation. In: XXII IMAC, Dearborn
15. Peairs DM (2006) High frequency modeling and experimental analysis for implementation of impedance-based structural health monitoring. PhD thesis, Virginia Polytechnic Institute and State University, Virginia, 150 pp
16. Raju V (1997) Implementing impedance-based health monitoring. PhD thesis, Virginia Polytechnic Institute and State University, Virginia, 224 pp
17. Park G, Kabeya K, Cudney HH, Inman DJ (1999) Impedance-based structural health monitoring for temperature varying applications. *JSME Int J* 42(2):249–258
18. Inman DJ, Farrar CR, Lopes V Jr, Steffen V Jr (2005) Damage prognosis: for aerospace, civil and mechanical systems. Wiley, England
19. Giurgiutiu V, Zagrai A (2005) Damage detection in thin plates and aerospace structure with the electro-mechanical impedance method. *Struct Health Monit* 4(2):99–118
20. Neto RMF, Steffen V Jr, Rade DA, Gallo CA, Palomino LV (2011) A low-cost electromechanical impedance-based SHM architecture for multiplexed piezoceramic actuators. *Struct Health Monit* 10(4):391–402